The Astrophysical Journal, 760:55 (7pp), 2012 November 20 doi:10.1088/0004-637X/760/1/55

A PRECISE PHYSICAL ORBIT FOR THE M-DWARF BINARY GLIESE 268

R. K. Barry[1], B.-O. Demory[2], D. Ségransan[2], T. Forveille[3], W. C. Danchi[1], E. Di Folco[2], D. Queloz[2], H. R. Spooner[4], G. Torres[5], W. A. Traub[6], X. Delfosse[3], M. Mayor[3], C. Perrier[3], and S. Udry[2]
[1] NASA Goddard Space Flight Center, Laboratory for Exoplanets and Stellar Astrophysics, Code 667, Greenbelt, MD 20771, USA; Richard.K.Barry@nasa.gov
[2] Massachusetts Institute of Technology, Cambridge, MA 02139, USA
[3] Geneva Observatory, Geneva University, 51 Ch.des Maillettes, CH-1290 Versoix, Switzerland
[4] University of Maryland, College Park, MD 20742, USA
[5] Harvard-Smithsonian Center for Astrophysics, 60 Garden Street, Cambridge, MA 02136, USA
[6] Jet Propulsion Laboratory, California Institute of Technology, Pasadena, CA 91109, USA
Received 2012 August 30; accepted 2012 October 9; published 2012 November 2

ABSTRACT

We report high-precision interferometric and radial velocity (RV) observations of the M-dwarf binary Gl 268. Combining measurements conducted using the IOTA interferometer and the ELODIE and Harvard Center for Astrophysics RV instruments leads to a mass of $0.22596 \pm 0.00084\ M_{\odot}$ for component A and $0.19230 \pm 0.00071\ M_{\odot}$ for component B. The system parallax as determined by these observations is 0.1560 ± 0.0030 arcsec—a measurement with 1.9% uncertainty in excellent agreement with *Hipparcos* (0.1572 ± 0.0033). The absolute *H*-band magnitudes of the component stars are not well constrained by these measurements; however, we can place an approximate upper limit of 7.95 and 8.1 for Gl 268A and B, respectively. We test these physical parameters against the predictions of theoretical models that combine stellar evolution with high fidelity, non-gray atmospheric models. Measured and predicted values are compatible within 2σ. These results are among the most precise masses measured for visual binaries and compete with the best adaptive optics and eclipsing binary results.

Key words: stars: general – stars: individual (Gliese 268) – techniques: interferometric – techniques: radial velocities

Online-only material: color figures

1. INTRODUCTION

Many stellar parameters are strongly dependent on mass, which, for most stars, must be inferred from age, metallicity, and luminosity. While techniques such as microlensing may be used to determine the mass of individual stars, the most practical approach for precision measurement, given current technology, is determination of masses of the components of multiple systems when the physical orbit is known. Evolutionary models take this mass as input and must reproduce the effective temperature and luminosity of both components under the assumption that the component stars are coeval and of the same metallicity (e.g., Baraffe et al. 1998; Andersen 1991). In this way, mass determinations may be used to calibrate mass–luminosity (ML) relations and evolutionary models. Visual (spatially resolved, non-eclipsing) binaries allow determination of stellar mass and absolute magnitudes in parts of the H-R diagram unpopulated by rare eclipsing binaries. This is of particular importance for low-mass stars.

At the low-mass end of the main sequence are the M-dwarf stars. These are distinctly underrepresented in studies that have made precise determinations of stellar mass. This may be surprising given their numbers, as the initial mass function gives the distribution of the number of stars of different masses as being inversely proportional to mass (Kroupa 2002). Although these objects are quite numerous, they are intrinsically faint with luminosities falling in the range 10^{-2}–$10^{-4}\ L_{\odot}$ (Reid & Hawley 2005). Moreover, their small sizes relative to their orbital separations mean that M-dwarf binary systems will display eclipses only very rarely. They are of great scientific interest since, unlike other types of stars on the main sequence, mid-to-late M-dwarfs are fully convective. Moreover, evolutionary models for M-dwarf stars are already known to show discrepancies with observations, especially for close binaries (Torres & Ribas 2002), and a recent study by Chabrier et al. (2007) suggests significant deviations from single-star models when applied to short-period binaries. Characterization of non-eclipsing binaries, in particular, is important to help to understand new evidence that short-period, synchronized binaries may have a different mass–radius relation than slower rotating single stars or stars in wide binaries. In Morales et al. (2010), for instance, the authors describe measurements of close binaries that appear to follow the accepted ML relations while the stellar radii are different than predicted. The measurements we describe below may prove helpful in resolving this new challenge to theory.

Evolutionary models and ML relations that have been calibrated may then be used to determine masses of individual stars and to correct stellar luminosity functions and star formation theories under the assumption that single stars have the same properties as stars in detached binary systems. Theoretical models have advanced to the point that the effective temperature and luminosity estimates they produce do not show diagnostic value until relative mass errors are below about 2% (e.g., Andersen 1991; Forveille et al. 1999). ML relations are well established and calibrated for solar-type stars for which extensive calibration has been conducted, but not for low-mass stars. This is especially true for the very low mass end where stars begin to be fully convective, have low-temperature electron degeneracy in their cores, and have complex atmospheres dominated by molecular opacity (Delfosse et al. 2000). Moreover, molecular opacity sources for these stars are typically described by theoretical line lists that are incomplete, resulting in decreased model fidelity. Consequently, an independent check of ML relations for low-mass, main-sequence stars is highly desirable.

Measurement of the masses of low-mass, main-sequence stars is important for another reason as well. Frequently, stars that host planets are isolated and mass must be determined through observation of the star's luminosity and color—resulting in a strong reliance on the ML relations. Any indeterminacy in the mass of the exoplanet's host star strongly couples in to measurement of planetary mass, bulk density, and other important characteristics. Recent discoveries of extra-solar planets orbiting nearby low-mass stars (Delfosse et al. 1998a; Marcy et al. 1998; Charbonneau et al. 2009; Carter et al. 2011; Muraki et al. 2011; Bonfils et al. 2011) have highlighted an urgent need to calibrate the appropriate ML relations.

Because there is a strong observational bias against observing eclipses in small, faint stars, M-dwarfs in particular are underrepresented in surveys for which the objective is calibration of ML relations. While masses for solar-type stars have been calculated with less than 1% indeterminacy, M-dwarf visual binaries are in the 1%–3% range (Ségransan et al. 2000; Irwin et al. 2009). Additionally, well-detached eclipsing M-dwarf binaries fill the H-R diagram quite poorly. Until quite recently, the only known detached eclipsing M-dwarf binaries were YY Gem (Forveille et al. 1999), CM Dra (Metcalfe et al. 1996), and GJ 2069a (Delfosse et al. 1999). All three of these systems' host stars are chromospherically active due, primarily, to the relatively high rotation rate of their component stars. There is evidence that YY Gem, in particular, is highly maculated (Torres & Ribas 2002). As a result, all three have slightly redder colors than expected for single stars of comparable bolometric luminosity. The evolution of these short-period eclipsing binary systems may also be affected by tidally induced rotational mixing. As a result, these stars may not be representative of isolated stars and, consequently, may not be good calibrators for low-mass stellar evolution models. Recently, as byproducts of planetary transit searches, there are now more M-dwarf eclipsing binaries known (Becker et al. 2008; Blake et al. 2008); however, these new binaries are much fainter and their parameters are not yet well determined.

For these compelling reasons, it is important to find additional systems in the low-mass regime for which masses and luminosities can be accurately determined in order to constrain models. The double-lined spectroscopic M-dwarf binary, Gliese 268 (*HIP34603*, $\alpha = 7^{\rm h}10^{\rm m}01\overset{\rm s}{.}83$, $\delta = 38^\circ31'45\overset{''}{.}1$, $J2000.0$), is just such a system. First, it is reasonably bright in the H band at an approximate magnitude of $m_H = 6.152$, even though it is faint in the V band at $m_V = 11.47$, making it an observable target for some long-baseline interferometers operating in the near-infrared. Gl 268 is spectroscopically categorized as an M4.5 dwarf system (Reid et al. 1995). The *Hipparcos* parallax of the Gl 268 system is 157 mas (6.38 pc) (van Leeuwen 2007), and the component semimajor axes are $a\sin(i) \simeq 0.29$ & 0.35 AU, based on the ∼10.4 day orbital period (Tomkin & Pettersen 1986). Second, because the derived radii of the individual spectroscopically categorized dwarfs are a negligible fraction of their separation, this system is likely to be fully detached, making it a good test system for modeling of single-star astrophysics. Third, the Gl 268 system has narrow absorption lines indicating that each of the elements of the binary are slowly rotating. Observations of late-type, short-period, dwarf binary stars (Andersen 1991) indicate that most will become tidally locked. We may infer from this that the average $V\sin(i) = 4$ km s^{-1} is an upper limit to the rotationally broadened line widths measured. Although there is evidence that stars with low rotational velocity are unlikely to be highly maculated (Delfosse et al. 1998b), the light from Gl 268 is variable, strongly suggesting starspots. Furthermore, it is identified in both the General Catalog of Variable Stars (Kukarkin et al. 1971) and the catalog of Chromospherically Active Binary Stars (Strassmeier et al. 1988). It is also listed as a flare star and a soft X-ray source in both the Einstein (McDowell 1994) and *ROSAT* (Voges et al. 2000) catalogs. While its activity and likely maculation may increase errors in the determination of the velocity orbital components, the relative narrowness of emission lines in its spectrum has the opposite effect.

We used previously obtained radial velocity (RV) data from the ELODIE spectrograph (Baranne et al. 1996) to calculate approximate component masses, $m_{1,2}\sin^3(i) \sim 0.18$. Comparing this to the mass prediction ($m_{1,2}\sin^3(i) \sim 0.2$) obtained using the roughly linear empirical function between mass and magnitude (Chabrier & Baraffe 1997; Henry & McCarthy 1993) suggests that the orbital inclination must be close to 90°—nearly edge-on—making Gl 268 ideal in this respect. This makes the fitted mass values less sensitive to errors in this parameter. These facts make Gl 268 suitable for constraining low-mass evolutionary models.

Until now, accurate masses for M-dwarf stars were derived principally either from eclipsing binaries, for which the inclination angle is unambiguous, or from combined RV and adaptive optics (AO) observations of non-eclipsing binaries. Here, we present combined interferometric and RV observations that yield masses at the 0.4% precision level. For the remainder of this paper, we describe the observations (Section 2), the orbit analysis (Section 3), and a summary of our conclusions (Section 4).

2. OBSERVATIONS AND DATA REDUCTION

When the orbits are not perfectly edge-on, one may only find the absolute masses of the component stars by extracting the unknown projection factor, $\sin(i)$, in some way. AO, speckle interferometry, or pupil masking interferometry on a large, filled-aperture telescope, or long-baseline, sparse-aperture interferometry are observational techniques that can be exploited to enable such observations. For example, Boden & PTI Collaboration (1997) used the Palomar Testbed Interferometer (Colavita et al. 1995) together with RV data to determine physical orbits for four short-period binaries while Hummel et al. (1998) used the Navy Precision Optical Interferometer (Hutter et al. 1993). Ségransan et al. (2000) derived the mass characteristics and, in some cases, the distances of 16 low-mass binary stellar systems by combining highly accurate velocity data with AO images. The images obtained for that work allowed highly accurate size measurements of the targets because the telescope was used near its theoretical diffraction-limited spatial resolution. Recent advances in stellar long-baseline interferometry allow the possibility of making extremely precise astrometric measurements of the motion of binaries in the tangent plane of the sky. We describe our RV and astrometric measurements of the Gl 268 system below.

2.1. Radial Velocity Measurements

We conducted extensive observations of Gl 268 at the Observatoire de Haute Provence, Saint Michel l'Observatoire, France using the ELODIE instrument on the 1.93 m telescope and the Harvard Center for Astrophysics (CfA) spectrograph on the 1.5 m Wyeth reflector at the Oak Ridge Observatory, Massachusetts, USA. The ELODIE fiber-fed echelle

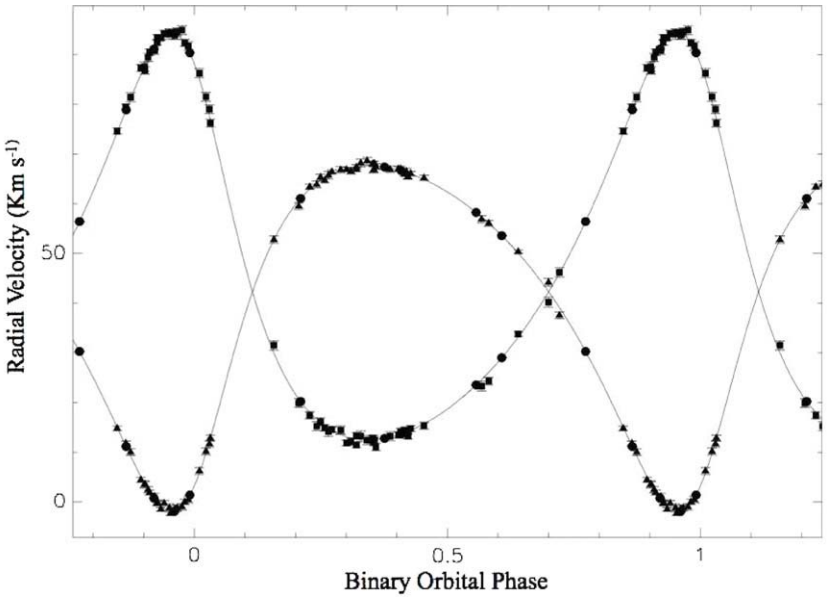

Figure 1. Orbit of the M-dwarf binary Gl 268 as fitted to individual velocity data points measured at the 1.5 m Wyeth reflector at the Oak Ridge Observatory, Massachusetts, USA (triangles: primary star; squares: secondary) and the Observatoire de Haute Provence, Saint Michel l'Observatoire, France using the ELODIE instrument (round dots).

spectrograph in a single exposure can record a spectrum at a resolution of $R = 42{,}000$ over a bandpass from 3906 Å to 6811 Å on a 1024×1024 CCD (Baranne et al. 1996). The accuracy and efficiency of the instrument together with its long-term stability admit the measurement of RV with an accuracy of better than 15 m s^{-1} for stars up to 9th magnitude in V while it is also capable of measuring velocities to about 1 km s^{-1} for stars up to 16th magnitude depending on spectral type. Data were immediately processed with a system integrated with the spectrograph control software, which produces optimally extracted and wavelength-calibrated spectra. These algorithms and processes are described in Baranne et al. (1996). The CfA instrument is an echelle spectrograph operating at $R = 35{,}000$ providing a minimum resolution element of 8.5 km s^{-1} (Wyatt 1985; Latham 1985).

Of the total eleven RV correlation profiles obtained for this work, nine are described in Delfosse et al. (1999). We obtained two additional measurements using the ELODIE in 2003. The velocity data for the primary and secondary components of Gl 268 are plotted on a phase-wrapped velocity curve in Figure 1. Processing of the many individual observations to determine RV is described in detail in Delfosse et al. (1999).

2.2. Astrometric Measurements

We observed Gl 268 using the now-decommissioned Infrared and Optical Telescope Array (IOTA) at the F. L. Whipple Observatory, Arizona over a period of six months from 2005 October to 2006 April. IOTA had baselines between 5 and 38 m and fiber-fed IONIC3 combiner optics (Berger et al. 2003) which we used to measure three squared visibilities (V^2) and one closure phase (CP) simultaneously in the broadband H filter with $\lambda = 1.647$ μm and $\Delta\lambda = 0.3$ μm (Zhao et al. 2007). Data analysis procedures have been thoroughly documented (e.g., Monnier et al. 2004). For the data presented here, we have adopted a calibration error of $\triangle V^2 = 3\%$ as described below.

Although Gl 268 was observed for 11 epochs, four of them were dropped because the signal-to-noise ratio was low and atmospheric piston errors were large. Out of the seven remaining epochs, two additional nights were dropped because the calibrated coherence factor of one calibrator star, Gl 251, was found to change during the course of the observations. The shortest baseline was not used because the instrumental transfer function was poor. Consequently, CP measurements were not included in the analysis. Fortunately, we obtained sufficient calibrator data on relevant nights to allow recovery of the system transfer function. As a result, we gathered a total of 110 useful V^2 measurements over five nights. The V^2 measurements obtained using IOTA are plotted in Figure 2 superimposed on fitted V^2 curves for various epochs of observation as described in Section 3. OIFITS files of the IOTA observations will be made available upon request to the lead author.

2.3. Systematic Error

When reporting formal errors in calculated masses of astronomical sources that are below 1%, particularly for low-mass stars, the dominant sources of measurement error are likely to be systematic, although astrophysical effects must also be examined. In particular, cross-correlation line blending and the effects of stellar maculation bear on the final result and we are obliged to ensure that each effect is fully understood before we may assert that we have obtained an accurate measurement. Because of the rarity of binary stars that are suitable for this type of measurement and extreme paucity of the types of astronomical data necessary for the required calculations, fundamental properties of the successfully observed low-mass binaries are particularly important as a calibration for theoretical models. At the level of 1% uncertainty, as required for such calibration, the data must be examined with care for systematic errors that might bias the results, particularly the masses.

Line blending typically results in significant uncertainty in RV determinations. In particular, measurement error due to line blending is proportionally to the inverse square root of the number of lines used in the correlation analysis. This effect is greatly reduced in our observations by the very broad spectroscopic window granted us, by design, with the ELODIE instrument (Latham et al. 1996; Baranne et al. 1996). Moreover,

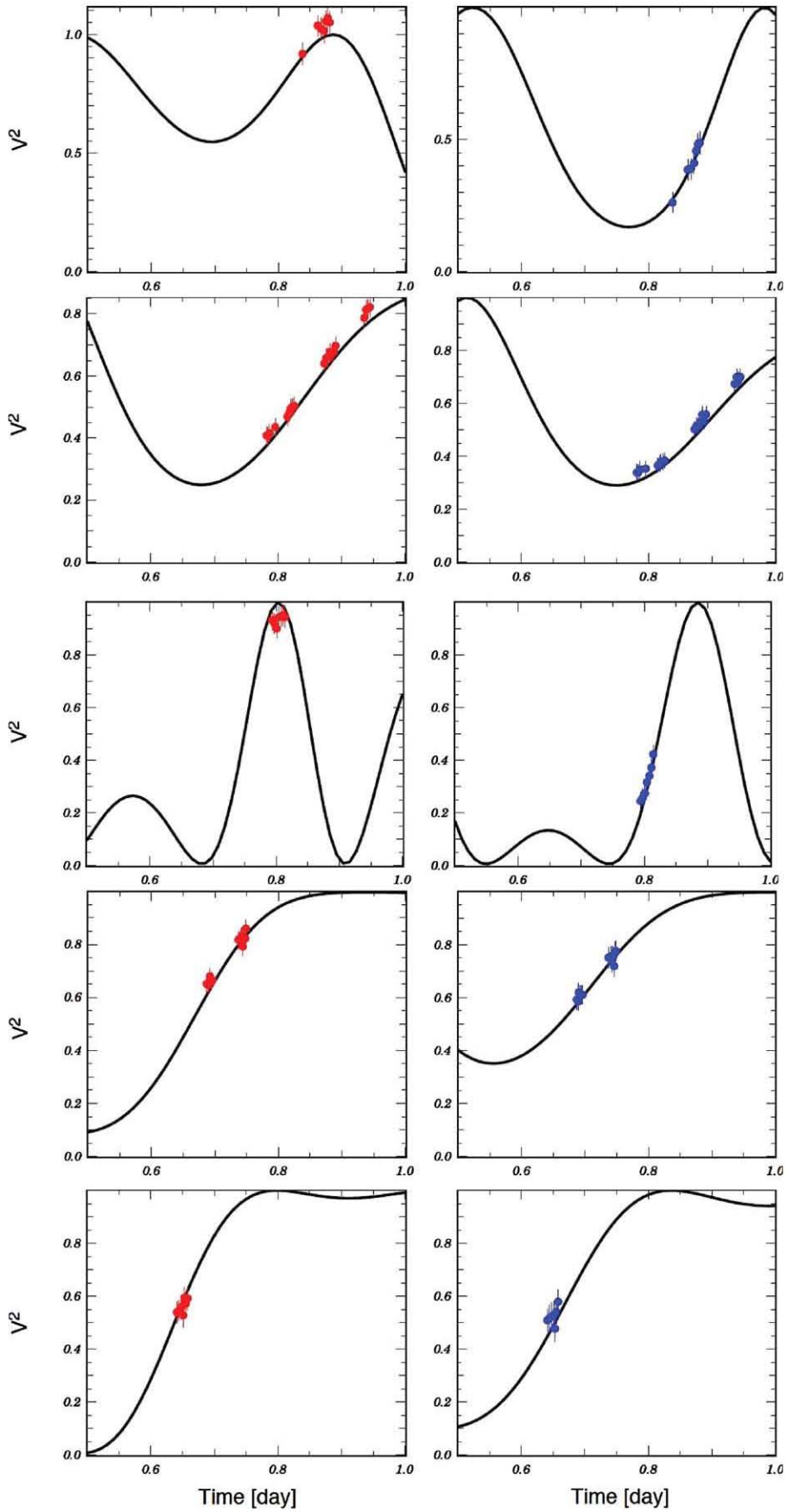

Figure 2. Visibility measurements of Gl 268 obtained using the IOTA interferometer. Measurements on baselines AB (left column) and BC (right column) are given as red and blue points, respectively, for JD 2453724, 2453726, 2453770, 2453799, and 2453837 from top to bottom. The abscissa of each is given as a fractional part of the JD date the measurement was taken.

(A color version of this figure is available in the online journal.)

we utilized a profile correction process, detailed by Forveille et al. (1999), in which systematic errors in the variation of the velocity curves due to line blending are reduced by a factor of approximately five.

As described by Delfosse et al. (1999) we analyzed the ELODIE echelle spectra by numerical cross correlation with an M4 V one-bit mask based on the spectrum of Barnard's star. Simply determining the RV by adjusting fitted double-Gaussians to the correlation profiles would have resulted in large systematic phase-dependent residuals. This is due to the fact that while the core of the correlation profiles are well described by a Gaussian distribution, their baselines do not drop to zero as a Gaussian function would. The measured baselines instead drop to about one-tenth of the depth of the secondary (fainter) star's correlation function dip. However, because of the good stability of the ELODIE spectrograph, the shape of the correlation profile for a given star is quite stable over time. This allows an estimate of the wings of the intrinsic correlation profile for each star by averaging all profiles obtained after aligning them at the measured velocity of the star. All pixels within two profile widths of the velocity of the companion star were blocked out. The residuals of the Gaussian adjustment to the average profiles are then subtracted from all correlation profiles at the velocity of each star. Forveille et al. (1999) evolved this procedure, which we applied to our data to successfully reduce the fluctuation level of the profile baseline to a level of approximately $\pm 0.05\%$. The rms change to the individual component velocities measured by double-Gaussian fitting compared to the application of this procedure are $\sim$18 ms^{-1} for the primary (brighter) and $\sim$25 ms^{-1} for the secondary (fainter) component as reported below.

Unlike Torres & Ribas (2002) we do not have direct light curve measurements of the Gl 268 system with which we can definitively rule out maculation, or to model it if detected. However, we do not anticipate that starspots, if they do exist on the components of Gl 268, will strongly affect our results for the following reasons.

The strength of dynamo processes in the outer envelopes of stars is strongly correlated with their rotational velocity. Line widths of the individual components of Gl 268 suggest that they are rotating at less than 5 km s^{-1}. Because of this slow rotation rate, the rotational shear, and consequently the magnetohydrodynamical generation of maculation, is expected to be negligible. Postulating a conservative equatorial velocity upper limit of $V_{Eq}\sin(i) = 2$ km s^{-1}, we calculate that we would require starspots covering 1% of the surface of each of the component stars of Gl 268 to induce shifts in the component velocity semi-amplitudes of 20 ms^{-1}, and fully 5% coverage, assuming a worst-case spot configuration, to induce shifts that reach the level of current mass errors. While $V_{Eq}\sin(i)$ cannot be predicted with great confidence based on these arguments, they do suggest that significant stellar maculation is not at issue for Gl 268. Moreover, starspots are unlikely to have remained stable over the many years of our RV measurements. Consequently, the errors that they produce may be considered as random rather than systematic.

We account for measurement errors in our astrometric observations at IOTA as follows. Each measurement of the V^2 we conducted is based on 100–200 individual interferogram scans. For statistical errors we report the ms scatter of these measurements. To this, we add a conservative estimate of the systematic error obtained from previous observations. For IOTA, previous observations of the very bright target, Vega, were determined to have a systematic error of $\triangle V^2 \sim 1\%$ (Defrère et al. 2011). For the particular case of Gl 268, a relatively faint target, we conservatively estimate a systematic error of 3%.

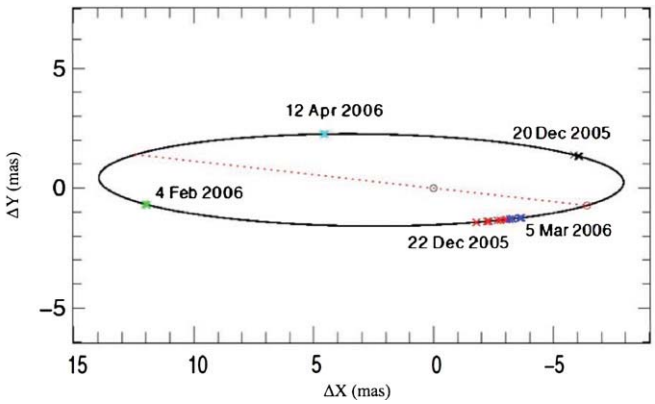

Figure 3. Derived physical orbit of the M-dwarf binary Gl 268 in the primary's frame of reference. Superimposed on the orbit are the predicted positions of secondary at the epoch of each of the interferometric measurements conducted at IOTA. Colors are used to discriminate observation dates as shown. The red dotted line is the line of nodes and the circle at the intersection of the line of nodes and the orbit ellipse is the secondary at periastron.

(A color version of this figure is available in the online journal.)

3. ORBIT ANALYSIS

The combination of RV and interferometric measurements permits reconstruction of the three-dimensional orbit and the binary system's flux ratio. Input data provided to our code are the 11 ELODIE correlation profiles (of 451 points each), the 58 CfA RV, and the 110 IOTA squared visibility measurements detailed in Section 2. Our code has the following set of free parameters: the eccentricity e, orbital period P, time of periastron T_0, the systemic velocities—the velocities of the barycenter of the system as measured by each of the Harvard, Center for Astrophysics (CfA), and ELODIE (ELO) instruments—$\gamma_{\rm CfA}$ and $\gamma_{\rm ELO}$, argument of periastron ω, the two semi-amplitudes K_1 and K_2, the longitude of ascending node Ω, the semimajor axis a, orbital inclination i, and the flux ratio q (Hilditch 2001).

Our minimization code is based on the Levenberg–Marquardt nonlinear least-squares fitting algorithm (Press et al. 1992). We use the publicly available Yorick implementation of the algorithm *lmfit*. Our binary model computes the RV for each star and the squared visibility of the system at each epoch for a given combination of the 12-parameter set described above. The RV part of the model is based on a simple Keplerian model of two stars orbiting their center of mass. The interferometric part of the model requires the computation of the Thiele–Innes (geometrical) coefficients to determine the position angle and separation of the system (Hilditch 2001). The smearing of the V^2 induced by the IOTA-IONIC bandwidth of 0.3μm is accounted for (Zhao et al. 2007; Charlassier et al. 2010). The code includes the array configuration and target coordinates for each epoch. The flux ratio, q, is then used to compute the squared visibility for each baseline. We estimate the standard deviation for all fitted parameters by performing 1000 bootstrap permutations on the data points.

The best-fit orbital parameters for Gl 268 along with their errors are shown in Table 1. The visual orbit resulting from this analysis is shown in Figure 3.

Table 1
Orbital and Binary Parameters of Gliese 268

Parameter	Tomkin & Pettersen (1986)	This Paper
Period (days)	10.428 ± 0.002	10.42672 ± 0.00006
V_0 (km s^{-1})	37.0 ± 0.003	41.792 ± 0.025
K_1 (km s^{-1})	32.5 ± 0.7	34.814 ± 0.036
K_2 (km s^{-1})	39.3 ± 0.5	40.874 ± 0.052
e	0.34 ± 0.02	0.3203 ± 0.0009
ω (deg)	217.7 ± 3.9	211.98 ± 0.19
Ω (deg)	...	89.98 ± 0.07
T_0 (JD − 2400000)	45770.8 ± 0.09	50493.9853 ± 0.0039
$a_1 \sin(i)$ (mas)	4.47 ± 0.13	4.726459 ± 0.0024
$a_2 \sin(i)$ (mas)	5.37 ± 0.25	5.556005 ± 0.0037
$M_1 \sin^3(i)$ ($M_\odot$)	0.191 ± 0.015	0.21530 ± 0.00024
$M_2 \sin^3(i)$ ($M_\odot$)	0.159 ± 0.011	0.18315 ± 0.00018
i (deg)	...	100.39 ± 0.03
a (mas)	...	11.10 ± 0.05
M_T ($M_\odot$)	...	0.419 ± 0.006
M_1 ($M_\odot$)[a]	...	0.226 ± 0.003
M_2 ($M_\odot$)[a]	...	0.193 ± 0.003
M_1 ($M_\odot$)[b]	...	0.22599 ± 0.00065
M_2 ($M_\odot$)[b]	...	0.19248 ± 0.00056
H-band flux fraction[c]	...	1.163 ± 0.021
π (arcsec)[d]	...	0.15888 ± 0.00072

Notes. A listing of the derived orbital and binary parameters of Gl 268. Subscripts refer to the stellar components of the system with component 1 being the more massive. We give the corresponding results from the work of Tomkin & Pettersen (1986) when available to show the improvements obtained through our new observations. These improvements are due, primarily, to significant advancements in the determination of radial velocity by Baranne et al. (1996).
[a] Assuming *Hipparcos* parallax.
[b] Assuming the parallax value determined in this study.
[c] H-band flux fraction given as flux1/flux2.
[d] *Hipparcos* parallax is 0.″15887 ± 0.″00335.

4. GL 268 AS A BENCHMARK FOR STELLAR EVOLUTION MODELS

4.1. Stellar Masses

Our global analysis of interferometric and RV data yield a precision of 0.4% on the individual stellar masses. The binary system's parallax measured by *Hipparcos* of 158.87 ± 3.35 mas is significantly improved by the constraints brought by the interferometric measurements. Our new parallax value of 158.88 ± 0.72 mas tightens the relative precision on the binary components masses from 1.4% to 0.4%, thus providing a true benchmark for stellar evolution models.

4.2. Flux Ratio

In addition to the determination of separation and position angle of the binary system, interferometric measurements also provide constraints on the components' flux ratio (see, e.g., Zhao et al. 2007). The CP, in which a sign change is induced when the observed binary system becomes unresolved in all baselines due to the system's stellar components' orbital motion about the barycenter, provides the most constraining input to the flux ratio. Our CP measurements, which we did not use in the orbit fitting procedure due to the poor transfer function in the shortest baseline, could yet have provided this constraint by localizing the sign change. Unfortunately, we were unable to conduct observations at the correct phase for this purpose. As a consequence, we rely on the flux ratio determination from the 110 squared visibilities measurements over five nights alone, yielding $q = (f1/f2) = 1.16 \pm 0.02$ and $\Delta_H = 0.16$. Here, as in Table 1, the subscripts refer to the individual stellar components of Gl 268 with component 1 being the more massive.

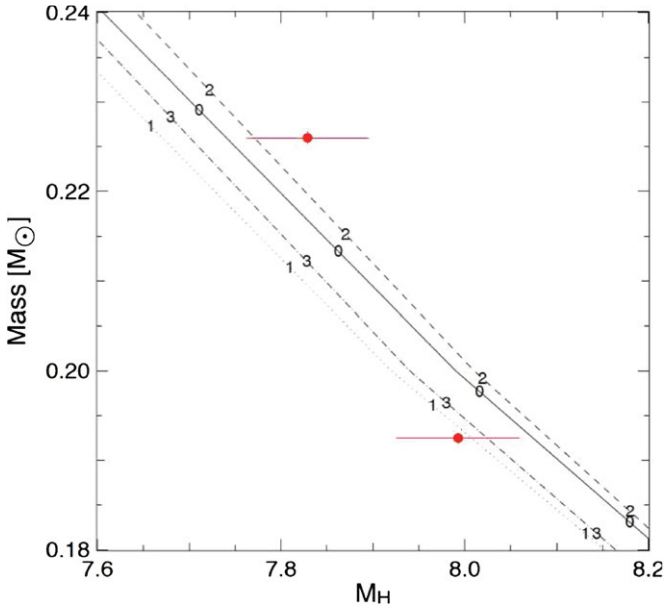

Figure 4. Derived parameters, with 1σ error bars, are shown for the M-dwarf binary Gl 268 compared to the prediction of a late-type stellar model (Baraffe et al. 1998). Abscissa is in units of absolute magnitude using Two Micron All Sky Survey photometry and our deduced parallax. The best fit, 10 Gyr isochrone (solid line, numeral 0) has a mixing length of 1H_p, helium abundance $Y = 0.275$, solar metallicity [Fe/H] = 0. Leaving all other parameters the same but changing the metallicity to [Fe/H] = −0.5 shifts the 10 Gyr isochrone toward the left (dotted, numeral 1). Changing the age to 5 Gyr causes both of these loci to move to the right—predicting slightly dimmer stars (dashed, numeral 2 for solar metallicity, dash-dot, numeral 3 for [Fe/H] = −0.5). Changes to mixing length (convection efficiency), helium abundance, metallicity, and age have little effect on the slope of the isochrones, suggesting the possibility that the model of (Baraffe et al. 1998) may not fully describe the underlying physics.
(A color version of this figure is available in the online journal.)

4.3. Comparison with Models

The flux ratio and stellar masses determined from our global analysis could be used to assess the agreement of our findings with the low-mass stellar evolutionary models from Baraffe et al. (1998).

Our results are shown in the H-band mass–magnitude plane on Figure 4, along with four models described in the figure caption. Here we show models with mixing length expressed in units of pressure scale height, H_P, to permit us to assess convection efficiency. Interestingly, the less massive component (component 2) seems to be better reproduced by low-metallicity models while solar metallicity is required to reproduce the most massive component (component 1). A word of caution is necessary, however, because of the error bars' amplitude of each component along the absolute magnitude axis. Better H-band photometry and a tighter constraint on the system's flux ratio are desirable to improve the significance of this comparison.

Although discrepancies are of the order of 2σ, we note that the observed lower mass-magnitude slope cannot be reproduced by changing helium abundance, Y, nor by adjustments in convection efficiency (mixing length). Changing age is not relevant for M-dwarfs such as Gl 268. Such stars effectively remain on the zero-age main sequence during their entire lifetime. Activity

effects are barely noticeable in the *H* band for this range of masses as they primarily affect radius rather than luminosity. In addition, the orbital period is sufficiently long to avoid tidal locking effects that would have induced an activity contribution observed in close systems (Chabrier et al. 2007).

The measured flux ratio in the *H* band for the component stars of Gl 268 as reported in Table 1 agrees with the sense of the masses determined by these measurements—with the greater mass corresponding to higher flux. Individual magnitudes are determined by this flux ratio, with the joint bolometric magnitude being fixed by the system parallax. As a consequence, the error bars of each component are strongly correlated—if the true luminosity is 1σ brighter for the primary, it is automatically 1σ fainter for the secondary. In this case, measurement and theoretical slope appear to be in reasonably good agreement. Notwithstanding this consideration, our inability to change the mass–magnitude *slope* to better fit both stellar components with one isochrone suggests that the luminosity difference between them, if real, may be due to physics that is not accounted for in the non-accreting stellar evolution model we tested.

5. CONCLUSIONS

The masses and absolute luminosities obtained for the M-dwarf binary Gl 268 by these measurements represent a new benchmark for precision measurements for M-dwarf visual systems. They provide an independent calibration of empirical ML relations and a needed check of the predictions of theoretical models of M-dwarf stellar physics (Chabrier & Baraffe 1997). As indicated above, Figure 4 depicts the mass and luminosity of the two components of Gl 268 together with the predictions of Baraffe et al. (1998). There appears to be reasonable agreement between our measurements and model predictions with discrepancies below the 2σ level. In particular, we note the theoretical ML relation appears to be insufficiently steep. This may be caused by an error in our measurement of magnitude difference between the component stars or an error in the theory. While the absolute magnitudes and masses we derive generally validate the evolutionary model we tested, our findings suggest some residual low-level departure from fidelity in the model or remaining small biases in flux ratio calibration.

We are grateful to the National Aeronautics and Space Administration, the University of Grenoble Observatory, Jet Propulsion Laboratory, the California Association for Research in Astronomy, and to the Harvard-Smithsonian Center for Astrophysics for support of this research. We are also grateful for the work on software to reduce the interferometric data from IOTA by J. Monnier. B.O.D. acknowledges the support of the *Fonds National Suisse de la Recherche Scientifique*. R.K.B. acknowledges the technical editing assistance of C. M. Morales Sabogal.

Facility: IOTA

REFERENCES

Andersen, J. 1991, A&A Rev., 3, 91
Baraffe, I., Chabrier, G., Allard, F., & Hauschildt, P. H. 1998, A&A, 337, 403
Baranne, A., Queloz, D., Mayor, M., et al. 1996, A&AS, 119, 373
Becker, A. C., Agol, E., Silvestri, N. M., et al. 2008, MNRAS, 386, 416
Berger, J.-P., Haguenauer, P., Kern, P. Y., et al. 2003, Proc. SPIE, 4838, 1099
Blake, C. H., Torres, G., Bloom, J. S., & Gaudi, B. S. 2008, ApJ, 684, 635
Boden, A. F., & PTI Collaboration. 1997, BAAS, 29, 1279
Bonfils, X., Gillon, M., Forveille, T., et al. 2011, A&A, 528, A111
Carter, J. A., Winn, J. N., Holman, M. J., et al. 2011, ApJ, 730, 82
Chabrier, G., & Baraffe, I. 1997, A&A, 327, 1039
Chabrier, G., Gallardo, J., & Baraffe, I. 2007, A&A, 472, L17
Charbonneau, D., Berta, Z. K., Irwin, J., et al. 2009, Nature, 462, 891
Charlassier, R., Bunn, E. F., Hamilton, J.-C., Kaplan, J., & Malu, S. 2010, A&A, 514, A37
Colavita, M. M., Hines, B. E., Wallace, J. K., et al. 1995, BAAS, 27, 1381
Defrère, D., Absil, O., Augereau, J.-C., et al. 2011, A&A, 534, A5
Delfosse, X., Forveille, T., Beuzit, J.-L., et al. 1999, A&A, 344, 897
Delfosse, X., Forveille, T., Mayor, M., et al. 1998a, A&A, 338, L67
Delfosse, X., Forveille, T., Perrier, C., & Mayor, M. 1998b, A&A, 331, 581
Delfosse, X., Forveille, T., Ségransan, D., et al. 2000, A&A, 364, 217
Forveille, T., Beuzit, J.-L., Delfosse, X., et al. 1999, A&A, 351, 619
Henry, T. J., & McCarthy, D. W., Jr. 1993, AJ, 106, 773
Hilditch, R. W. 2001, in An Introduction to Close Binary Stars, ed. R. W. Hilditch (Cambridge: Cambridge Univ. Press), 392
Hummel, C. A., Mozurkewich, D., Armstrong, J. T., et al. 1998, AJ, 116, 2536
Hutter, D. J., Elias, II, N. M., Hindsley, R. B., et al. 1993, BAAS, 25, 1405
Irwin, J., Charbonneau, D., Berta, Z. K., et al. 2009, ApJ, 701, 1436
Kroupa, P. 2002, in ASP Conf. Ser. 285, Modes of Star Formation and the Origin of Field Populations, ed. E. K. Grebel & W. Brandner (San Francisco, CA: ASP), 86
Kukarkin, B. V., Kholopov, P. N., Pskovskij, Y. P., et al. 1971, General Catalogue of Variable Stars, Vol. III (Moskva: Astronomical Council of the Academy of Sciences)
Latham, D. W. 1985, in IAU Colloq. 88, Stellar Radial Velocities, ed. A. G. D. Philip & D. W. Latham (Schenectady: L. Davis Press), 21
Latham, D. W., Nordstroem, B., Andersen, J., et al. 1996, A&A, 314, 864
Marcy, G. W., Butler, R. P., Vogt, S. S., Fischer, D., & Lissauer, J. J. 1998, ApJ, 505, L147
McDowell, (ed.) 1994, The Einstein Observatory Soft X-ray Source List
Metcalfe, T. S., Mathieu, R. D., Latham, D. W., & Torres, G. 1996, ApJ, 456, 356
Monnier, J. D., Traub, W. A., Schloerb, F. P., et al. 2004, ApJ, 602, L57
Morales, J. C., Gallardo, J., Ribas, I., et al. 2010, ApJ, 718, 502
Muraki, Y., Han, C., Bennett, D. P., et al. 2011, ApJ, 741, 22
Press, W. H., Teukolsky, S. A., Vetterling, W. T., & Flannery, B. P. 1992, Numerical recipes in C. The Art of Scientific Computing (Cambridge: Cambridge Univ. Press)
Reid, I. N., & Hawley, S. L. 2005, New Light on Dark Stars: Red Dwarfs, Low-mass Stars, BrownDwarfs (Berlin: Springer)
Reid, I. N., Hawley, S. L., & Gizis, J. E. 1995, AJ, 110, 1838
Ségransan, D., Delfosse, X., Forveille, T., et al. 2000, A&A, 364, 665
Strassmeier, K. G., Hall, D. S., Zeilik, M., et al. 1988, A&AS, 72, 291
Tomkin, J., & Pettersen, B. R. 1986, AJ, 92, 1424
Torres, G., & Ribas, I. 2002, ApJ, 567, 1140
van Leeuwen, F. 2007, A&A, 474, 653
Voges, W., Aschenbach, B., Boller, T., et al. 2000, IAU Circ., 7432, 3
Wyatt, W. F. 1985, in IAU Colloq. 88, Stellar Radial Velocities, ed. A. G. D. Philip & D. W. Latham (Schenectady: L. Davis Press), 123
Zhao, M., Monnier, J. D., Torres, G., et al. 2007, ApJ, 659, 626